Symposium on Materials Processing Under the Influence of Electrical and Magnetic Fields
2003 TMS Annual Meeting**, San Diego, Ca, March 2-6, 2003**

MAGNETIZED FIBER ORIENTATION AND CONCENTRATION CONTROL IN SOLIDIFYING COMPOSITES

George S. Dulikravich[1], Marcelo J. Colaço[1], Thomas J. Martin[2], Seungsoo Lee[3]

[1]University of Texas at Arlington, Mechanical & Aerospace Eng. Dept., MAIDO Institute;
UTA Box 19018; Arlington, TX 76019, USA
[2]Pratt & Whitney Engine Company, Turbine Discipline Engineering & Optimization Group;
400 Main Street, M/S 169-20; East Hartford, CT 06108, USA
[3]3-3-2, Agency for Defense Development: Youseong P.O. Box 35-3, Daejeon, KOREA

Abstract

A new concept for manufacturing specialty composite materials has been developed where a user-specified pattern of magnetic lines of force can be achieved so that micro fibers will align with this pattern. An improved analytical model and a numerical algorithm have been developed for the prediction of magnetic force lines inside a flowing and solidifying melt. This analysis code was combined with a hybrid constrained optimization algorithm that minimizes a normalized sum of least square differences between the user-specified and the predicted patterns of the magnetic lines of force. This software package was used to inversely evaluate the strengths, locations, and orientations of magnets needed to generate the user-specified pattern of the magnetic lines of force in the solidifying composite thus verifying the conceptual feasibility of this manufacturing process.

Introduction

It is well known that defects in short fiber composites are often due to uncontrolled fiber orientation and concentration during composites manufacturing (Cranston and Reitz, 1980). These defects can significantly reduce the functionality of the composite material (Hatta and Yamashita, 1988). Also, in many applications it would be highly desirable to have directional dependence of physical properties of the material, that is, to have strongly non-isotropic materials (Smith et al., 1996). This implies that it would be of interest to perform curing of the resin in such a way that the local concentration and orientation of the fibers is fully controlled. During a controlled solidification process from a melt, it is important to understand the process of solid phase formation. The accumulated solid phase effectively reduces and deforms the cross sectional area of the passages and causes significant local variations in pressure and melt flow-field shear stresses. During the solidification process, melt flow is generated due to strong thermal buoyancy forces. This process cannot be effectively controlled in the case of strong heat transfer, except if influenced by a global body force. One such body force is the general electromagnetic Lorentz force that is created in any electrically conducting fluid when either a magnetic field or an electric field is applied.

During the curing process in composites manufacturing, we usually work with electrically conducting liquid polymers and carbon fibers, although a variety of other molten substances and fibers made of other materials are often used. The resins are electrically conducting either because of the presence of iron atoms, salts, or acids. In addition, if short carbon fibers (5-10 microns in diameter and 200 microns long) are vapor-coated with a thin layer (2-3 microns) of a ferromagnetic material like nickel (Hatta and Yamashita, 1988), the fibers will respond to the externally applied electromagnetic fields by rotating and translating so that they become aligned with the magnetic lines of force (Hatta and Yamashita, 1988; Yamashita et al., 1989). This is especially true for short fibers (Hatta and Yamashita, 1988). Thus, if an external magnetic field is applied, the molten resin flow-field will respond and the solid/liquid front shape and its speed could be manipulated non-intrusively (Dulikravich, Kosovic and Lee, 1993; Dennis and Dulikravich, 2001; 2002).

The objective of this work is to explore the feasibility of manufacturing specialty metal matrix and polymer composite materials that will have specified (desired) locally directional variation of bulk physical properties like thermal and electrical conductivity, modulus of elasticity, thermal expansion coefficient, etc. The fundamental concept is based on specifying a desired pattern of orientations and spacing of micro fibers in the final composite material product. Then, the task is to determine the proper strengths, locations, and orientations of magnets that will have to be placed along the boundaries of the curing composite part so that the resulting magnetic field lines of force will coincide with the specified (desired) pattern of the micro fibers' distribution. The basic idea is that the fibers will align with the local magnetic lines of force (Hatta and Yamashita, 1988). It is important to understand that the pattern of these lines depends on the solidifying resin flow-field and the spatial variation of the applied magnetic field.

Thus, the successful proof of this manufacturing concept involves the development of an appropriate software package for the numerical solution of the partial differential equation system governing magneto-hydro-dynamics (MHD) involving combined fluid flow, magnetic field, and heat transfer that includes liquid-solid phase change (Dulikravich, 1999). In addition, it involves development of a constrained optimization software that is capable of automatically determining the correct strengths, locations, and orientations of a finite number of magnets that will produce the magnetic field force pattern which coincides with the desired and specified fiber concentration and orientation pattern in the curing composite material part.

Numerous analytical and numerical formulations have been developed for simulation of solidification processes in solidifying fluid flows with and without the influence of an externally applied steady magnetic field (Dulikravich, Kosovic, and Lee, 1993; Dulikravich, 1999). An extended form of the Boussinesq approximation allowing for temperature-dependent physical properties of the fluid including latent heat of phase change was incorporated in this formulation that simultaneously predicts detailed velocity, pressure, and temperature fields for the moving fluid while capturing the forming solid phase by using a single computer code. Computational results confirmed that the magnetic field has a profound influence on the solidifying flow-field. It reduces intensity of the flow recirculation (Dulikravich, Choi, and Lee, 1994; Dennis and Dulikravich, 2001; 2002) and causes distorted velocity profiles with pronounced overshoots

close to the solid boundaries. This change influences heat transfer through the boundaries and consequently the amount of the solid phase accrued on undercooled walls.

A Mathematical Model of Magneto-Hydro-Dynamics (MHD) With Solidification

The modifications to the Navier-Stokes relations for the MHD fluid flow with heat transfer and phase change come from the electro-magnetic force on the fluid where all induced electric field terms have been neglected. The latent heat released or absorbed per unit mass of mushy region (where $T_{liquidus} > T > T_{solidus}$) is proportional to the local volumetric liquid/(liquid + solid) ratio often modeled (Voller and Swaminathan, 1991) as

$$f = \frac{V_\ell}{V_\ell + V_s} = \left(\frac{T - T_{solidus}}{T_{liquidus} - T_{solidus}} \right)^n = \tilde{\theta}^n \tag{1}$$

Here, the exponent n is typically $0.2 < n < 5$, subscripts ℓ and s designate liquid and solid phases, respectively, while $f = 1$ for $T \geq T_{liquidus}$ and $f = 0$ for $T \leq T_{solidus}$. Physical properties (density, viscosity, heat conductivity, heat capacity, etc.) are often significantly different in the melt as compared to the solid phase. We may assume linear variation of density as a function of the non-dimensional temperature, θ, in the liquid

$$\rho_\ell = \rho_r \left[1 + \left(\frac{\partial(\rho_\ell / \rho_r)}{\partial \theta} \right)_r (\theta - \theta_r) \right] = \rho_r [1 - \alpha_\ell (\theta - \theta_r)] \tag{2}$$

with a similar expression for the solid phase. The reference values are designated with the subscript "r". Then, the liquid-solid mixture density and modified heat capacity can be defined as

$$\rho_{mix} = f\, \rho_\ell + (1 - f) \rho_s \tag{3}$$

$$c_{mix} = f \rho_\ell \frac{\partial \left(c_\ell\ \theta_\ell \right)}{\partial \theta} + (1 - f) \rho_s \frac{\partial \left(c_s^{eq}\ \theta_s \right)}{\partial \theta} \tag{4}$$

where an enthalpy method (Poirier and Salcudean, 1986) was used to formulate the equivalent specific heat coefficient in the solid phase defined as

$$c_s^{eq} = c_s - \frac{1}{S_{TE}} \frac{\partial L}{\partial \theta} \tag{5}$$

Here, Stefan number is defined as

$$S_{TE} = \frac{c_r \Delta T_r}{L_r} \tag{6}$$

so that latent heat, L_r, is released in the mushy region according to equation (5).

The remaining non-dimensional numbers are

Reynolds hydrodynamic	Prandtl hydrodynamic	Eckert
$R_e = \frac{\rho_r V_r \ell_r}{\mu_{vr}}$	$P_R = \frac{\mu_{vr} c_r}{\kappa_r}$	$E_C = \frac{V_r^2}{c_r \Delta T_r}$
Grashof	**Prandtl magnetic**	**Hartmann**
$G_R = \frac{\rho_r^2 \alpha_r g_r \Delta T_r \ell_r^3}{\mu_{vr}^2}$	$P_m = \frac{\mu_{vr} \sigma_r \mu_r}{\rho_r}$	$H_T = \ell_r \mu_r H_r \left(\frac{\sigma_r}{\mu_{vr}} \right)^{1/2}$

where $\mu_{vr}, c_r, \kappa_r, \mu_r, L_r, \ell_r, H_r, \sigma_r, \alpha_r$ are the reference values of viscosity, specific heat, heat conductivity, magnetic permeability, latent heat of liquid-solid phase change, length, magnetic field, electric conductivity, and thermal expansion, respectively. Then, the non-dimensional Navier-Stokes equations for phase-changing mixtures of two liquids (solid phase is treated as the second liquid with extremely high viscosity), can be formulated (Dulikravich and Lynn, 1995; Ko and Dulikravich, 2000; Dulikravich, 1999) so that the mixture mass conservation is

$$\nabla \cdot \underline{v} = 0 \tag{7}$$

where $\underline{v}$ is the fluid velocity. Linear momentum conservation for two-phase MHD flows with thermal buoyancy and magnetic force

$$\rho_{mix} \frac{\partial \underline{v}}{\partial t} + f \rho_\ell \nabla \cdot \left(\underline{v}\underline{v} + \hat{p}_\ell \underline{\underline{I}} \right) + (1-f) \rho_s \nabla \cdot \left(\underline{v}\underline{v} + \hat{p}_s \underline{\underline{I}} \right)$$

$$= f \left\{ \nabla \cdot \left[\frac{\mu_{v\ell}}{R_e} \left(\nabla \underline{v} + (\nabla \underline{v})^* \right) \right] + \frac{G_R}{R_e^2} \rho_\ell \alpha_\ell \theta \ \underline{g} + \frac{H_T^2}{P_m R_e^2} \mu_\ell (\nabla \times \underline{H}) \times \underline{H} \right\} \tag{8}$$

$$+ (1-f) \left\{ \nabla \cdot \left[\frac{\mu_{vs}}{R_e} \left(\nabla \underline{v} + (\nabla \underline{v})^* \right) \right] + \frac{G_R}{R_e^2} \rho_s \alpha_s \theta \ \underline{g} + \frac{H_T^2}{P_m R_e^2} \mu_s (\nabla \times \underline{H}) \times \underline{H} \right\}$$

The non-dimensional hydrodynamic, hydrostatic, and magnetic pressures were combined to give

$$\hat{p}_\ell = \frac{p}{\rho_\ell} + \frac{\varphi}{F_R^2} + \frac{H_T^2}{P_m R_e^2}\mu_\ell \underline{H}\cdot\underline{H} \qquad \text{and} \quad \hat{p}_s = \frac{p}{\rho_s} + \frac{\varphi}{F_R^2} + \frac{H_T^2}{P_m R_e^2}\mu_s \underline{H}\cdot\underline{H} \tag{9}$$

where φ is the non-dimensional gravity potential defined as $\underline{g} = -\nabla\varphi$. Then, the energy conservation for incompressible phase-changing MHD flows including Joule heating can be written in its non-dimensional form as (Dulikravich, 1999)

$$c_{mix}\frac{\partial\theta}{\partial t} + f\rho_\ell \nabla\cdot\left(c_\ell \theta \underline{v}\right) + (1-f)\rho_s \nabla\cdot\left(c_s^{eq}\theta\underline{v}\right) = f\left[\frac{1}{R_e P_R}\nabla\cdot\left(\kappa_\ell\nabla\theta\right) + \frac{1}{\sigma_\ell}\frac{H_T^2 E_c}{P_m^2 R_e^3}\left(\nabla\times\underline{H}\right)\cdot\left(\nabla\times\underline{H}\right)\right]$$

$$+ (1-f)\left[\frac{1}{R_e P_R}\nabla\cdot\left(\kappa_s\nabla\theta\right) + \frac{1}{\sigma_s}\frac{H_T^2 E_c}{P_m^2 R_e^3}\left(\nabla\times\underline{H}\right)\cdot\left(\nabla\times\underline{H}\right)\right] \tag{10}$$

The classical modeling of MHD assumes that there are no free electric charges in the fluid (Dulikravich and Lynn, 1995; Ko and Dulikravich, 2000). With these assumptions Maxwell's system for electro-magnetics of a moving media becomes

$$\nabla\cdot\underline{B} = 0 \tag{11}$$

$$\nabla\times\underline{H} = \underline{J} \tag{12}$$

$$\nabla\cdot\underline{J} = 0 \tag{13}$$

Here, $\underline{H} = \underline{B}/\mu_o - \underline{M}$ is the magnetic field intensity, $\underline{B}$ is the magnetic flux density, $\underline{M}$ is the total magnetization per unit volume, μ_o is the magnetic permeability of vacuum. Ohm's law, which relates the induced electric current to the electric intensity vector, and the magnetic intensity vectors in a moving media, is given by

$$\underline{J} = \sigma\left(\underline{E} + \underline{v}\times\underline{B}\right) + \underline{v}q_e \tag{14}$$

Here, $\underline{J}$ is the electric current density, q_e is the total or free electric charge per unit volume and σ is the electric conductivity. If electric conductivity and magnetic permeability are assumed constant, then the following non-dimensionalized magnetic field transport equation for the phase-changing MHD flow can be obtained from equations (11)-(14). It needs to be solved intermittently (Dulikravich, 1999) with the equations (7-10).

$$\frac{\partial\underline{H}}{\partial t} - \nabla\times\left(\underline{v}\times\underline{H}\right) = \frac{f/\left(\sigma_\ell\mu_\ell\right) + (1-f)/\left(\sigma_s\mu_s\right)}{P_m R_e}\nabla^2\underline{H} \tag{15}$$

The modified magnetic transport equations (15), the continuity equation (7), the modified Navier-Stokes equations (8), and the modified energy equation (10) were integrated numerically using a finite volume method for structured grids written in terms of non-orthogonal boundary-conforming coordinates (Dulikravich, Ahuja and Lee, 1993). Artificial density formulation was used to de-singularize the Navier-Stokes system and the artificial time integration was performed using a four-stage Runge-Kutta algorithm.

Inverse Problem of Determining Unknown Magnetic Field Boundary Conditions

Given a prescribed pattern of magnetic field lines, let us try to estimate the magnetic field boundary conditions that will generate such a pattern. This is a typical inverse boundary condition determination problem (Dulikravich, Martin and Dennis, 1999). Because of the highly coupled system of non-linear partial differential equations governing the MHD solidification, the easiest approach to solving this problem is to formulate it as a least squares problem and then use an optimization algorithms to minimize the L-2 norm. Thus, the objective function for this problem could be the sum of all squared differences between the estimated and prescribed magnetic field components. The task is then to find the minimum of F, where F is defined as

$$F = \left[\frac{1}{\#\,\text{cells}} \sum_{i=1}^{\#\,\text{cells}} \left(B_x^{\text{specified}} - B_x^{\text{calculated}} \right)^2 + \frac{1}{\#\,\text{cells}} \sum_{i=1}^{\#\,\text{cells}} \left(B_y^{\text{specified}} - B_y^{\text{calculated}} \right)^2 \right]^{1/2} \qquad (16)$$

since magnetization was neglected in this work. The values of the magnetic field strength throughout the domain depend strongly on the values of the magnetic field along the boundaries of the domain. Thus, the desired pattern of the magnetic field lines could be created by the yet unknown boundary values of the magnetic field. Therefore, the boundary values of the magnetic field were parameterized with the following expression

$$B(x_k) = \sum_{i=1}^{M} P_i \; C_i \; (x_k) \qquad (17)$$

where the P_i's are unknown parameters that will be found with the help of the hybrid optimization algorithm. The functions $C_i(x_k)$ are given as

$$C_i(x_k) = \cos\left[(i-1)\frac{\pi}{2} x_k \right] \quad \text{for } i = 1,3,5,... \qquad (18)$$

$$C_i(x_k) = \cos\left[i\frac{\pi}{2} x_k \right] \quad \text{for } i = 2,4,6,... \qquad (19)$$

A variety of optimization algorithms have been developed and widely used in multiple disciplines. Various optimization algorithms have been known to provide faster convergence over others depending upon the size and shape of the mathematical design space, the nature of the constraints, and where they are during the optimization process. This is why we created a

hybrid constrained optimization software (Dulikravich, Martin, Dennis, and Foster, 1999) which incorporates several of the most popular optimization modules; the Davidon-Fletcher-Powell (DFP) gradient search method, a genetic algorithm (GA), the Nelder-Mead (NM) simplex method, quasi-Newton algorithm of Pshenichny-Danilin (LM), differential evolution (DE), and sequential quadratic programming (SQP). Each algorithm provides a unique approach to optimization with varying degrees of convergence, reliability, and robustness at different stages during the iterative optimization process. A set of analytic rules and heuristics were coded into the program to automatically switch back and forth among the different optimization algorithms as the process proceeded. Different versions of this hybrid optimization package have been successfully applied during the optimization of various multi-disciplinary problems (Dulikravich, Dennis, Martin and Egorov, 2002).

Numerical Results

Three test cases were considered corresponding to three different prescribed magnetic field boundary conditions. In all test cases the initial guess for the parameters is zero, that is, the initial guess for the magnetic field is that it is zero. The hybrid optimizer started with the Differential Evolutionary method in all test cases and the initial population was randomly generated around the initial guess. The number of population members was equal to three times the number of parameters. Input parameters used in all three test cases are given in Table I.

Table I. Input values

l = 0.01 m	Fr = 8.7870×10^{-2}
B_0 = 0.1 T	Ec = 7.1524×10^{-8}
Re = 1000	Ht = 4.1864×10^{1}
Pr = 1.1613×10^{-2}	Gr = 1.8132×10^{5}
V_0 = 2.7522×10^{-2} m/s	Ra = 2.1464×10^{2}

In test case 1 we used 3 parameters for $B_1(y)$ and 3 parameters for $B_3(x)$. Equation (17) was used to generate prescribed boundary conditions, where the values of the parameters P_i were

$$P_1 = 0.0032 \qquad P_2 = 0.0563 \qquad P_3 = 0.2365 \qquad P_4 = 0.3658 \qquad P_5 = 0.0698 \qquad P_6 = 0.0023$$

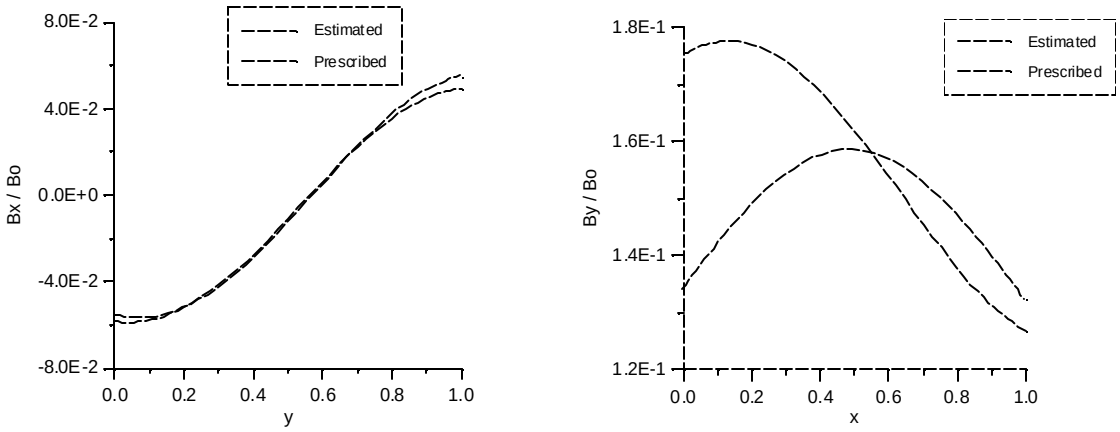

Figure 1. Specified and estimated boundary conditions for test case 1.

Figure 1 shows the estimated and prescribed boundary conditions for test case 1. One can see that the boundary conditions for $x = 0.0$ and $x = 1.0$ are better estimated than the boundary conditions for $y = 0.0$ and $y = 1.0$. Figure 2 shows the magnetic and temperature fields obtained with the prescribed boundary conditions (Figure 1) for test case 1.

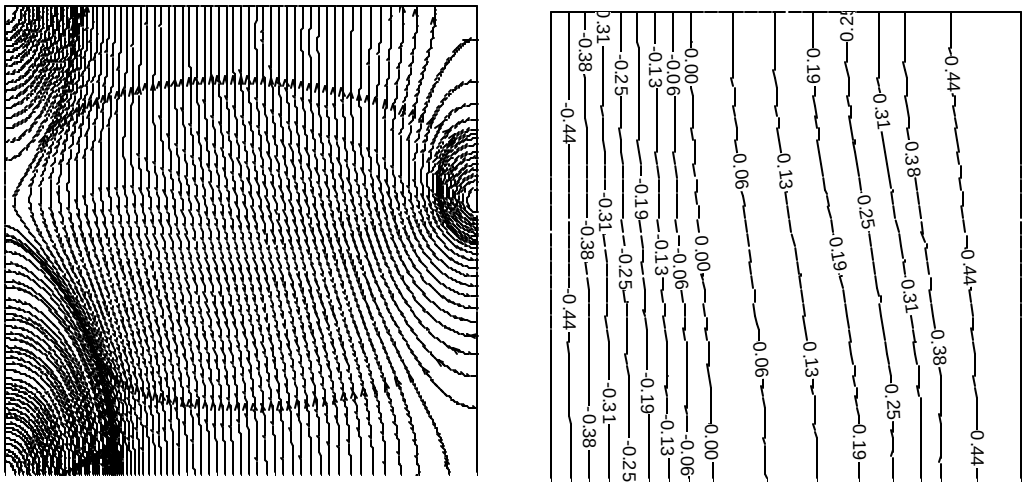

Figure 2. Specified magnetic and temperature field distributions for test case 1.

Figure 3 shows the estimated magnetic and temperature fields for test case 1 obtained from minimization of the objective function F (Eq. 16) with the use of a hybrid optimizer which varied the parameters of the boundary conditions of the magnetic field (Eq. 17). One can see that the magnetic and thermal fields obtained from this inverse methodology match the prescribed magnetic and thermal field patterns shown in Figure 2 very closely. Since all values are non-dimensionalized, the value of 0.0 in the thermal field plot designates the liquid/solid interface. Finally, Figure 4 shows the convergence history of the optimization process. In this case, the major optimization modules applied were the GA and the SQP modules.

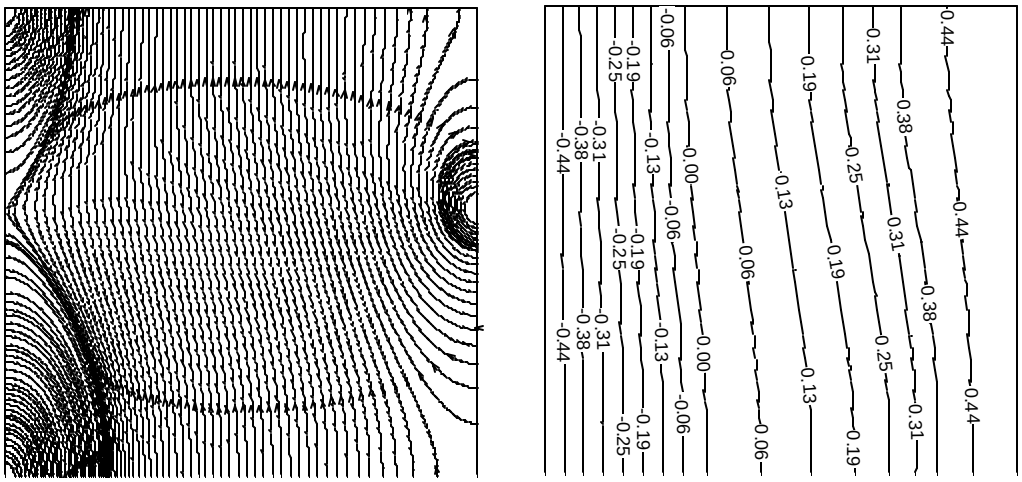

Figure 3. Calculated magnetic and temperature field distributions for test case 1.

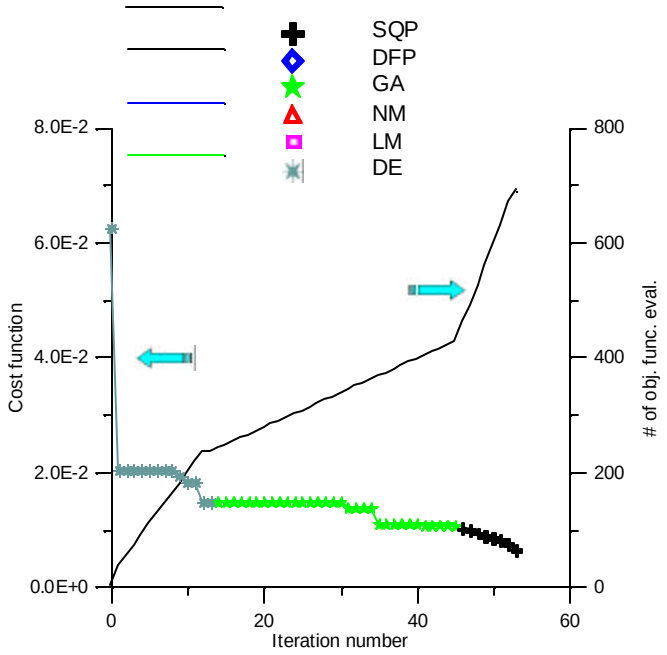

Figure 4. Convergence history for the hybrid optimization in test case 1.

Figure 5 shows the estimated and prescribed boundary conditions for test case 2, where a discontinuous function was considered. In this case, six parameters for $B_1(0,y)$ and six parameters for $B_3(x,0)$ were used, while boundary conditions on the opposite walls were enforced as periodic, that is $B_2(1,y) = B_1(0,y)$ and $B_4(x,1) = B_3(x,0)$. Again, the boundary conditions for $x = 0.0$ and $x = 1.0$ are better estimated than the boundary conditions for $y = 0.0$ and $y = 1.0$. The discontinuity at the boundary condition for $x = 0.0$ and $x = 1.0$ could be better estimated if more parameters were used for the trial functions given by Eq. (17). Figure 6 shows the magnetic and temperature field distributions obtained with the specified boundary conditions (Figure 5) for test case 2.

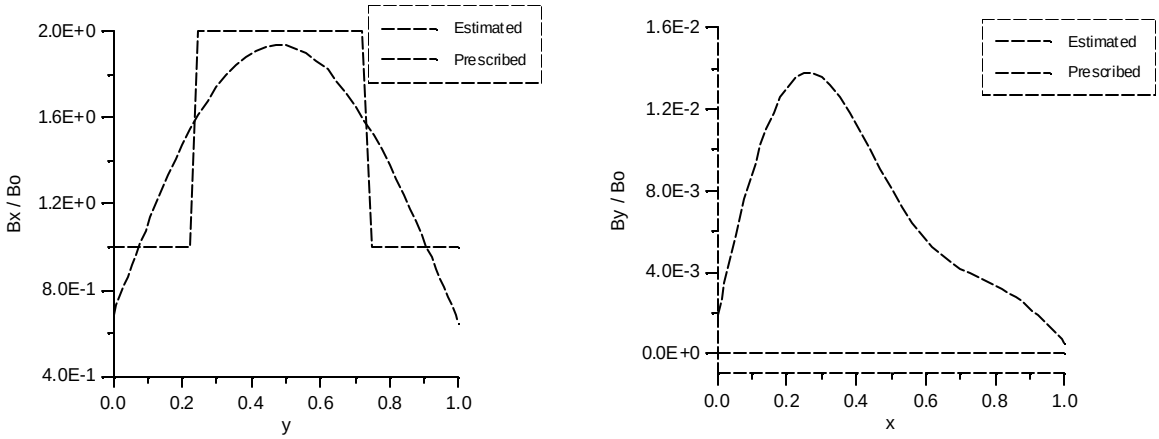

Figure 5. Specified and estimated boundary conditions for magnetic field in test case 2.

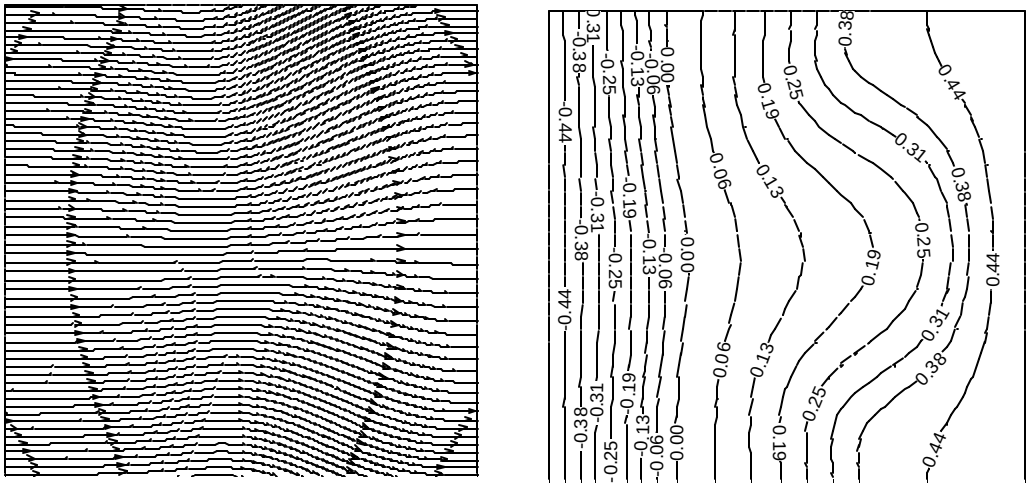

Figure 6. Specified magnetic and temperature field distributions for test case 2.

Figure 7 shows the estimated magnetic and temperature fields distribution for test case 2. One can see that they have the same shape of the prescribed fields depicted in Figure 6, except for the magnetic lines close to the boundaries $y = 0.0$ and $y = 1.0$. Figure 8 shows the convergence history, where one can see that the DE optimization module did not have a satisfactory performance in this case. In fact, for this case, the major optimization module was the GA.

It should be pointed out that these test cases used physical properties for silicon. The exception was the magnetic Prandtl number for which a value, which is three orders larger than the physical value, was used. This was done because the realistic extremely small values of P_m were causing the explicit numerical integration algorithm used in the MHD analysis to diverge. In addition, the value of viscosity coefficient in the solid phase was treated as only two orders of magnitude higher than in the liquid. Higher values of this artificial viscosity were causing the MHD analysis code to oscillate. As a result of using the lower values of the viscosity in the locally solidified locations, the local velocities predicted in the solid phase were not negligible. They needed to be explicitly re-initialized to zero values after each iterative sweep through the computational domain. This slowed the convergence rate of the MHD analysis significantly.

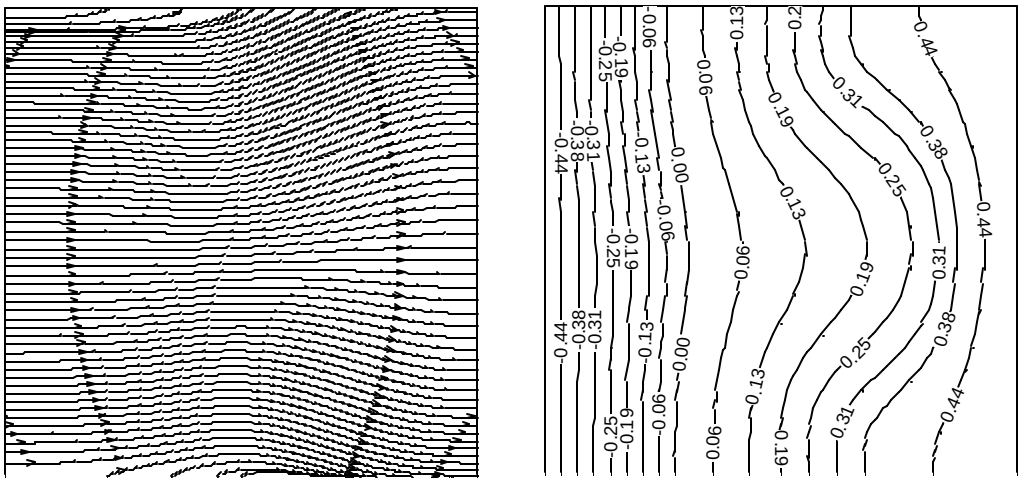

Figure 7. Calculated magnetic and temperature field distributions for test case 2.

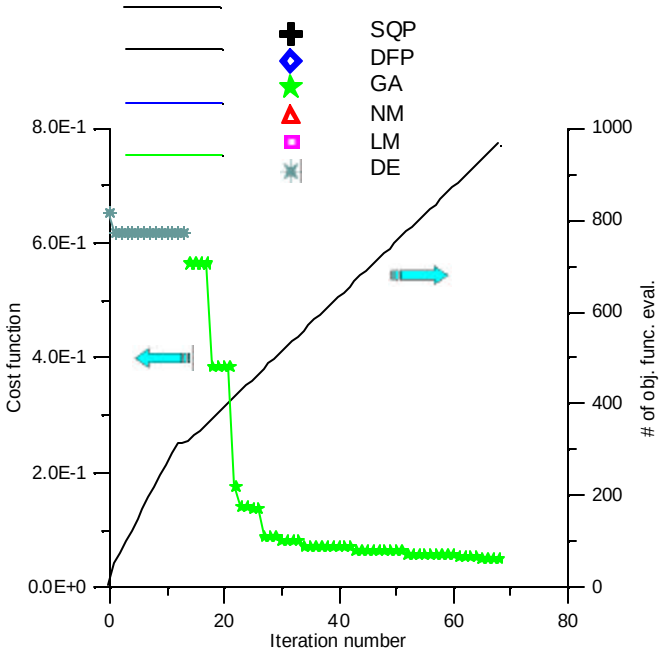

Figure 8. Convergence history for the hybrid optimization in test case 2.

For the case 3, the following problem was considered, using the same parameters of Table I.

Here (Figure 9), $T_c = 1676.0\,K$ and $T_h(x) = 4\left(-x^2 + x\right) + 1686.0\,K$. Figure 10 shows the estimated and the prescribed boundary conditions for test- case 3. In this case, three parameters were used for each of the four boundary conditions, where $B_1(0,y) \neq B_2(1,y)$ and $B_3(x,0) \neq B_4(x,1)$. That is, magnetic field boundary conditions were not explicitly treated as periodic. Figure 11 shows the prescribed magnetic and temperature field patterns obtained with the magnetic field boundary conditions as specified in Figure 10. Figure 12 shows the estimated

patterns of these fields obtained by optimizing 3 x 4 = 12 parameters describing the boundary values of the magnetic field. The specified and the optimized patterns of the magnetic and temperature fields match each other well.

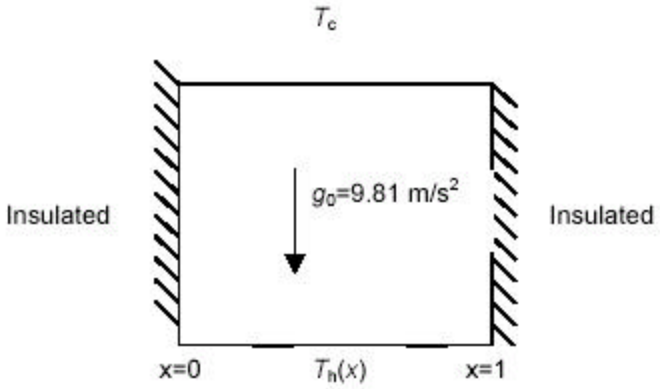

Figure 9. Normalized geometry and thermal boundary conditions for test case 3.

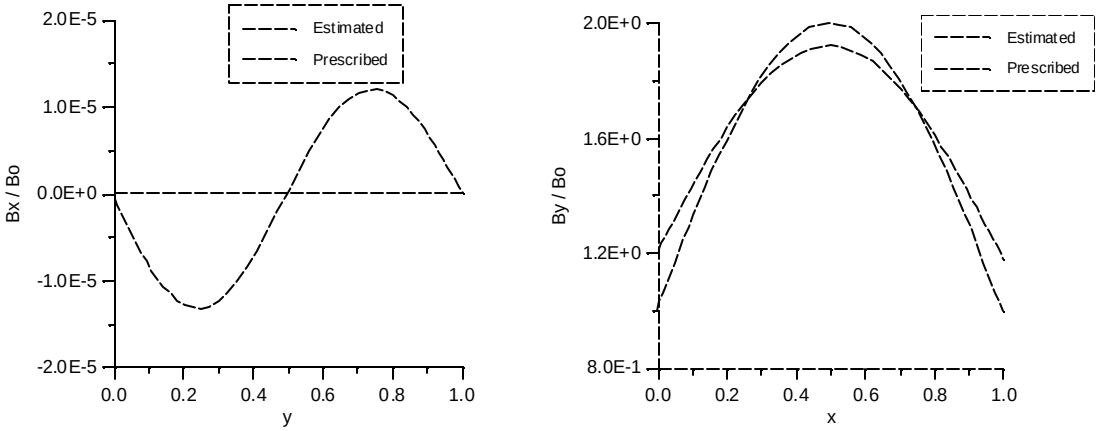

Figure 10. Specified and estimated boundary conditions for magnetic field in test case 3.

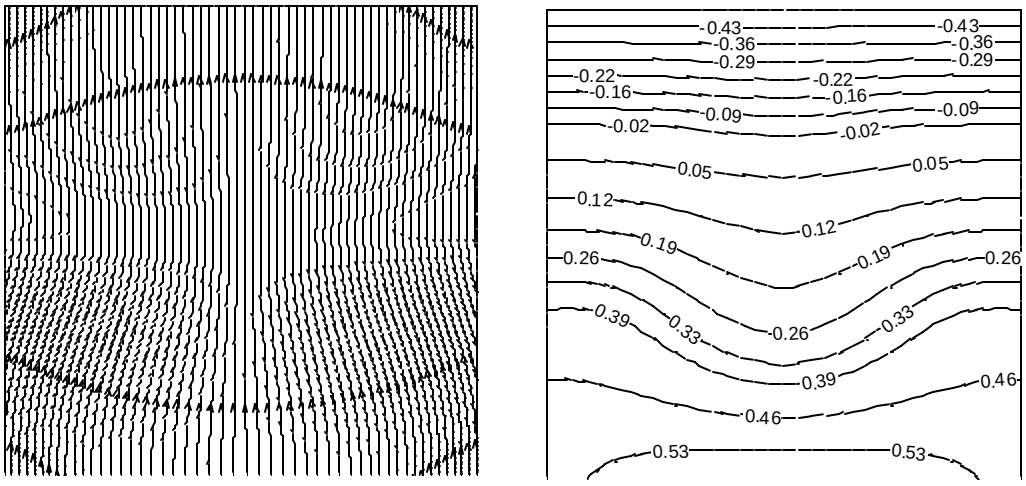

Figure 11. Specified magnetic and temperature field distributions for test case 3.

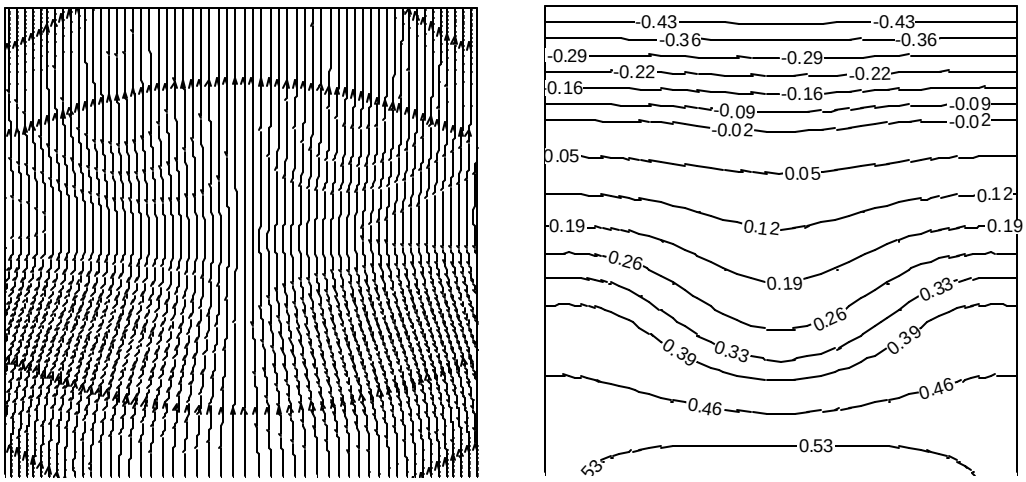

Figure 12. Calculated magnetic and temperature field distributions for test case 3.

Finally, Figure 13 shows that the SQP optimization module performed the entire task in case 3.

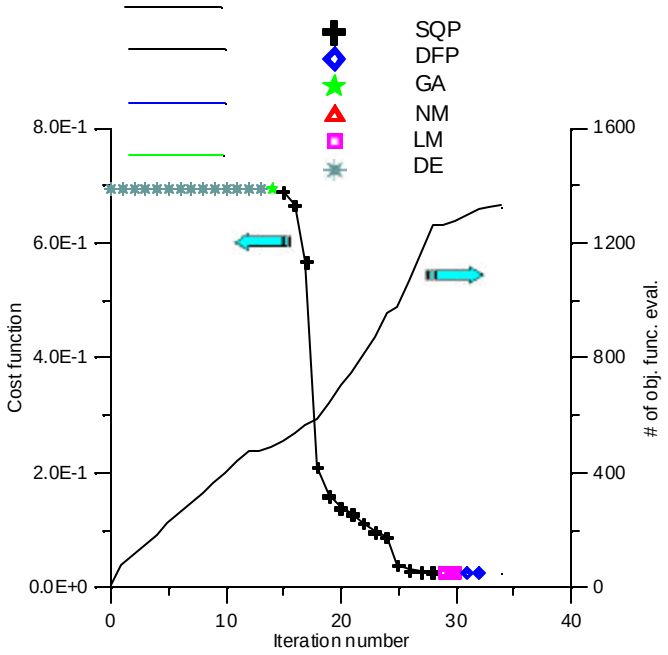

Figure 13. Convergence history for the hybrid optimizer for test case 3.

Discussion

In this proof-of-the-concept effort the objective was not to develop the most advanced MHD analysis involving solidification. The objective was to demonstrate the feasibility of the entire concept of inversely determining the unknown boundary values of the magnetic field that will create a user-specified pattern of the magnetic lines of force. In this study, a number of

assumptions were made concerning physics of the problem. For example, all physical properties were treated as constants instead of as functions of temperature. Transport equation for the passive scalar (concentration of the micro fibers) was not included, but could be added relatively easily (Hirtz and Ma, 2000). Its addition would enable us to predict and possibly control the distribution of the micro-fibers along the magnetic field lines of force. Thermal stresses in the accrued solid were not analyzed since such solids are by definition non-isotropic. Different options for treating the mushy region were not exercised (Poirier and Salcudean, 1986). Other, possibly more robust and accurate numerical integration methods were not explored (Fedoseyev et al., 2001; Dennis and Dulikravich, 2002) that could allow for physical values of the magnetic Prandtl number and for significantly higher values of viscosity used in the solid region. Magnetization effects and fiber-resin interface drag were neglected. Also, possible effects of the material properties and the thickness and shape of the container walls were not included via a conjugate analysis (Dennis and Dulikravich, 2000). All of these details could and should be incorporated in the future work and compared to actual experimental results since this concept could be extended to manufacturing of three-dimensional composite objects of arbitrary shape.

Summary

Feasibility of a new concept has been demonstrated for manufacturing composite materials where micro fibers will align along a user-specified desired pattern of the magnetic lines of force. This was accomplished by combining an MHD analysis code capable of simultaneously capturing features of the melt flow-field and the accrued solid, and a hybrid constrained optimization code. The computed pattern of the magnetic lines of force was shown to closely replicate the specified pattern when the optimizer minimized the L-2 norm of the difference between these two patterns. This minimization process was achieved by optimizing a finite number of parameters describing analytically the distribution and the orientations of the boundary values of the magnetic field.

Acknowledgements

The second author is grateful for the postdoctoral fellowship received from University of Texas at Arlington and from CNPq, a Brazilian council for scientific and technological development.

References

Cranston, J. J. and Reitz, J. A.III, 1980, "SMC Molding Techniques for Optimized Mechanical Properties in Structural Applications," *Polymer and Plastics Technology and Engineering*, Vol. 15, pp. 97-114.

Dennis, B. H. and Dulikravich, G. S., 2000, “Simulation of Magnetohydrodynamics With Conjugate Heat Transfer,” ECCOMAS2000 (European Congress on Computational Methods in Applied Sciences and Engineering), (ed: Onate, E., Bugeda, G. and Suarez, B.), Barcelona, Spain, September 11-14, 2000.

Dennis, B. H. and Dulikravich, G. S., 2001, "Optimization of Magneto-Hydrodynamic Control of Diffuser Flows Using Micro-Genetic Algorithm and Least Squares Finite Elements," *Journal of Finite Elements in Analysis and Design*, Vol. 37, No. 5, pp. 349-363

Dennis, B. H. and Dulikravich, G. S., 2002, "Magnetic Field Suppression of Melt Flow in Crystal Growth," *International Journal of Heat & Fluid Flow*, Vol. 23, No. 3, pp. 269-277.

Dulikravich, G. S., 1999, "Electro-Magneto-Hydrodynamics and Solidification," Chapter no. 9 in Advances in Flow and Rheology of Non-Newtonian Fluids, Part B (ed. D.A. Siginer, D. De Kee and R.P. Chhabra), Rheology Series, 8, Elsevier Publishers, June 1999, pp. 677-716.

Dulikravich, G. S. and Lynn, S. R., 1995, "Unified Electro-Magneto-Fluid Dynamics (EMFD): A Survey of Mathematical Models," *International Journal of Non-Linear Mechanics*, Vol. 32, No. 5, September 1997, pp. 923-932.

Dulikravich, G. S., Ahuja, V. and Lee, S., 1993, "Three-Dimensional Control of Crystal Growth Using Magnetic Fields," SPIE paper 1916-07, Proc. of Smart Structures and Materials Conf., Albuquerque, New Mexico, February 1-4, 1993.

Dulikravich, G. S., Ahuja, V. and Lee, S., 1994, "Modeling Three-Dimensional Solidification With Magnetic Fields and Reduced Gravity," *International Journal of Heat and Mass Transfer*, Vol. 37, No. 5, pp. 837-853.

Dulikravich, G. S., Choi, K.-Y. and Lee, S., 1994, "Magnetic Field Control of Vorticity in Steady Incompressible Laminar Flows," Symposium on Developments in Electrorheological Flows and Measurement Uncertainty 1994, ASME WAM'94, ed: D. A. Siginer, J. H. Kim, S. A. Sheriff and H. W. Colleman, Chicago, IL, Nov. 6-11,1994, ASME FED-Vol. 205/AMD-Vol. 190, pp. 125-142.

Dulikravich, G. S., Dennis, B. H., Martin, T. J. and Egorov, I. N., 2002, "Multi-disciplinary Design Optimization," *Invited Lecture*, EUROGEN 2001 - Evolutionary Methods for Design, Optimization and Control with Applications to Industrial Problems, (ed.: Giannakoglou, K., Tsahalis, D. T., Periaux, J. and Fogarty, T.), Athens, Greece, Sept. 19-21, 2001, Published by International Center for Numerical Methods in Eng. (CIMNE), Barcelona, Spain, pp. 11-18.

Dulikravich, G. S., Kosovic, B. and Lee, S., 1993, "Magnetized Fiber Orientation Control in Solidifying Composites: Numerical Simulation," *ASME Journal of Heat Transfer*, Vol. 115, pp. 255-262.

Dulikravich, G. S., Martin, T. J. and Dennis, B. H., 1999, "Multidisciplinary Inverse Problems," *Invited Lecture*, 3rd International Conference on Inverse Problems in Engineering (3icipe): Theory and Practice, ed. K. Woodbury, Port Ludlow-Puget Sound, WA, June 13-18, 1999; ASME Engineering Foundation Publications, pp.1-8.

Dulikravich, G. S., Martin, T. J., Dennis, B. H. and Foster, N. F., 1999, "Multidisciplinary Hybrid Constrained GA Optimization," Invited lecture, Chapter 12 in EUROGEN'99 - Evolutionary Algorithms in Engineering and Computer Science: Recent Advances and Industrial Applications, ed. K. Miettinen, M. M. Makela, P. Neittaanmaki and J. Periaux, John Wiley & Sons, Jyvaskyla, Finland, May 30 - June 3, 1999, pp. 233-259.

Fedoseyev, K. I., Kansa, E. J., Marin, C. and Ostrogorsky, A. G., 2001, "Magnetic Field Suppression of Semiconductor Melt Flow in Crystal Growth: Comparison of Three Methods for Numerical Modeling," Japanese *CFD Journal*, no. 9, pp. 325 - 333.

Hatta, H. and Yamashita, S., 1988, "Fiber Orientation Control by Means of Magnetic Moment," *Journal of Composite Materials*, Vol. 22, May, pp. 484-500.

Hirtz, J. M. and Ma, N., 2000, "Dopant Transport During Semiconductor Crystal Growth: Axial versus Transverse Magnetic Field," *J. of Crystal Growth*, Vol. 210, pp. 554-572.

Ko, H.-J. and Dulikravich, G. S., 2000, "A Fully Non-Linear Model of Electro-Magneto-Hydrodynamics," *International J. of Non-Linear Mechanics*, Vol. 35, No. 4, pp. 709-719.

Poirier, D. and Salcudean, M., 1986, "On Numerical Methods Used in Mathematical Modeling of Phase Change in Liquid Metals," ASME paper 86-WAM/HT-22, Anaheim, California, December 7-12, 1986.

Smith, M. E., Benicewicz, B. C., Douglas, E. P., Earls, J. D. and Priester, R. D. Jr., 1996, "Effect of High Magnetic Fields on Orientation and Properties of Liquid Crystalline Thermosets," *Polym. Prepr*. (Am. Chem. Soc., Div. Polym. Chem.), Vol. 37, No. 1, pp.50-1.

Voller, V. R. and Swaminathan, C. R., 1991, "General Source-Based Method for Solidification Phase Change," *Numerical Heat Transfer, Part B*, Vol. 19, pp. 175-189.

Yamashita, S., Hatta, H., Sugano, T. and Murayama, K., 1989, "Fiber Orientation Control of Short Fiber Composites: Experiment," *Journal of Composite Materials*, Vol. 23, pp. 32-41.